

Advanced Techniques for Grating Lobe Reduction for Large Deployable Mesh Reflector Antennas

Jakob Rosenkrantz de Lasson,
Cecilia Cappellin, and Rolf Jørgensen
TICRA
Copenhagen, Denmark
jrld@ticra.com

Leri Datashvili
LSS GmbH
Garching, Germany
leri.datashvili@largespace.de

Jean-Christophe Angevain
ESA-ESTEC
Noordwijk, The Netherlands
Jean.Christophe.Angevain@esa.int

Abstract—Spaceborne deployable mesh reflectors are lightweight antennas made by a tensioned net supporting an RF reflecting mesh, which are deployed in orbit. The tensioned net is typically made by regular and periodic planar triangles that cause unwanted grating lobes in the pattern of the antenna. Here, we build on a recent study and propose an improved configuration using a so-called pentagonal arithmetic mesh of non-regular and non-periodic triangles and a shifted feed that modifies the reflector phase distribution and simultaneously provides excellent grating lobe reduction and lowered sidelobes. This configuration may pave the way for future space missions relying on large deployable mesh reflector antennas.

I. INTRODUCTION

Large deployable reflector antennas receive significant attention in these years as lightweight alternatives to conventional solid reflectors for use in future space missions [1]. Inherent to these deployable reflectors is the use of planar triangles to approximate the otherwise smooth reflector surface, which degrades the associated RF performance, e.g. causing lower antenna gain. Additionally, if uniform triangles are used to form the tensioned net, radiation patterns exhibit grating lobes (GLs), that may limit the usefulness of deployable antennas in telecom and Earth observation missions [2], [3].

Using irregular tensioned net configurations is a means to degrade the GLs [4], and in [3] we reported a study of several of these types. The so-called arithmetic mesh [2], in which the mesh side length is gradually increased in an arithmetic series from the center and towards the edge, yielded the largest GL reduction (GLR), but presented an unwanted high first sidelobe. In this paper, we build on those findings and propose an arithmetic mesh configuration with a different symmetry, where a shift of the feed yields a phase distribution that, in addition to GLR, leads to an improved sidelobe distribution.

II. STRUCTURE

We consider an offset reflector with projected aperture diameter $D = 12$ m, focal length $f/D = 0.7$, and clearance $d' = 1.5$ m at a frequency of 1.4 GHz. We use a Gaussian feed with a 12 dB taper at the reflector edge, linearly polarized along the symmetry axis. This setup is illustrated in Fig. 1.

A given mesh reflector is constructed by distributing node points in the projected aperture (x, y) plane (shown in Fig. 1). The associated z coordinates lie on the paraboloidal surface,

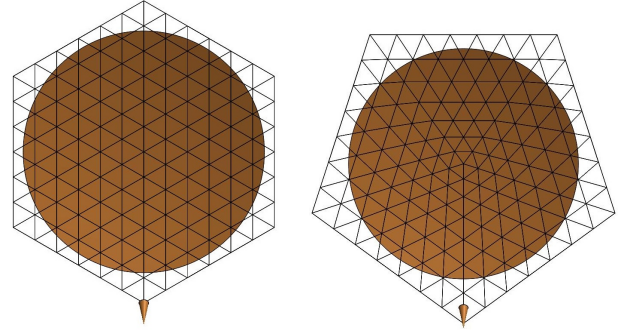


Fig. 1. Offset paraboloidal reflector with feed shown at bottom. *Left*: Uniform hexagonal mesh. *Right*: Arithmetic pentagonal mesh.

$z_i = (x_i^2 + y_i^2)/(4f)$, and are connected by planar triangles. So except at the node positions, the mesh reflector surfaces deviate from the nominal paraboloid.

III. NUMERICAL RESULTS

A. Nominal paraboloid and uniform mesh

All results are obtained with simulations in the GRASP software [5]. In Figure 2, the co-polar pattern in the H-plane ($\phi = 90^\circ$) is shown, with the pattern produced by the nominal paraboloid in black with a peak directivity of 43.85 dBi. For a uniform mesh with hexagonal symmetry (equilateral triangle side length = 1250 mm, 85 nodes, left in Fig. 1), we obtain the pattern shown in blue. In addition to a slight decrease of the peak directivity (43.74 dBi), this mesh reflector exhibits the characteristic GLs around $|\theta_{GL}| = 11.4^\circ$, in agreement with the theoretical prediction [3], and at 27.18 dBi below peak.

To investigate the GLs systematically, we consider for each configuration an azimuth and elevation far-field grid and from this subtract the nominal paraboloid envelope grid. Global maxima in these difference grids quantify the strength of GLs, and the smaller this difference, the smaller the GLs [3]. The uniform hexagonal mesh gives GLs with such a difference of 23.88 dBi, see Table I.

B. Arithmetic meshes

Inherent to the arithmetic mesh is a discrete rotational symmetry, and in [3] we considered hexagonal meshes. Inspired by [4], we have now in addition considered a pentagonal mesh,

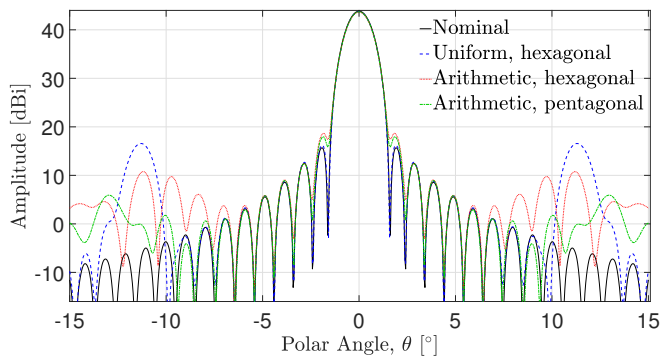


Fig. 2. Co-polar radiation patterns in the H-plane ($\phi = 90^\circ$).

TABLE I
MAXIMUM GRATING LOBE (AZ, EL) GRID DIFFERENCE.

	Nomi.	Uni., hex.	Arith., hex.	Arith., pent.	Arith., pent., CS.	Arith., pent., FS.
Max. grating lobe diff. [dBi]	0	23.88	15.99	14.23	17.69	14.85

shown to the right in Fig. 1 (91 nodes). In Fig. 2, the red (green) curve is the pattern for the hexagonal (pentagonal) arithmetic mesh. The pentagonal mesh yields the lowest GLs, see Table I, and is thus better for GLR. A similar investigation for uniform meshes (not shown here) supports this conclusion.

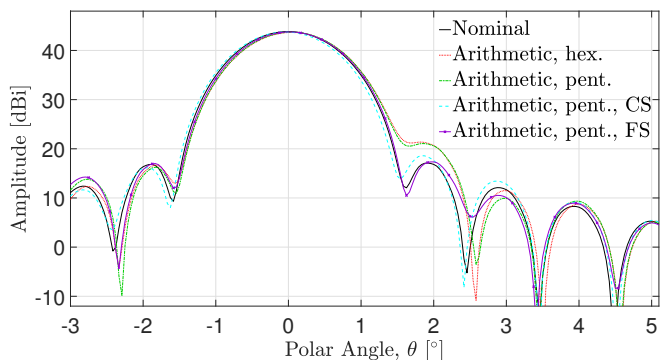


Fig. 3. Co-polar radiation patterns in the E-plane ($\phi = 0^\circ$).

A drawback of the arithmetic meshes is the relatively large first sidelobe that they give rise to [2], [3]. In Fig. 3, we show co-polar radiation patterns in the E-plane ($\phi = 0^\circ$). Both the hexagonal (red) and pentagonal (green) arithmetic meshes give a first sidelobe around $\theta = 1.8^\circ$ that is almost 4 dBi above the level of the nominal paraboloid. This large first sidelobe is due to a large phase variation towards the apex of the offset reflector where relatively large triangles are used to represent the most curved part of the surface. In the left panel of Fig. 4, the phase of the reflected electric field across the reflector is shown for the pentagonal arithmetic mesh, and the large phase variation towards the apex (bottom of figure) is apparent.

To remedy this, we shift the center of the arithmetic mesh from the center of the projected aperture and $D/4$ down towards the apex, in order to decrease the size of the triangles where the reflector curvature is largest. This setup (88 nodes) gives the dashed turquoise curve in Fig. 3 (CS), that indeed

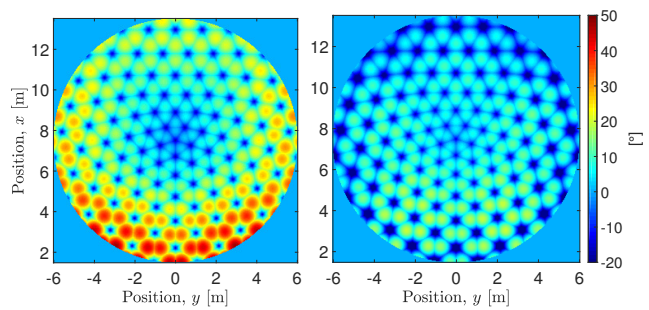


Fig. 4. Phase of reflected electric field for pentagonal arithmetic mesh. Left: Feed in focal point of nominal paraboloid. Right: Feed shifted 100 mm closer to the reflector.

exhibits a lower first sidelobe. At the same time, however, the GL increases by more than 3 dBi, see Table I.

Until now, the feed has been positioned in the focal point of the nominal paraboloid. The arithmetic mesh reflector is, however, slightly more curved than the nominal paraboloid, meaning that it has a slightly smaller focal length. As an additional investigation, therefore, we have returned to the center-expanded pentagonal arithmetic mesh and shifted the feed by $\Delta z = 100$ mm along the feed axis, closer to the reflector. This setup produces the pattern shown in purple in Fig. 3 (FS) with a first sidelobe that is essentially as low as for the nominal paraboloid. The associated phase distribution is shown in the right part of Fig. 4, and it is apparent that the phase varies less than with the nominal feed position. Equally important, the GLR only degrades by 0.6 dBi compared to the value obtained with the feed at the nominal focal point, see Table I. These are very promising results, and a configuration with force equilibrium in the tensioned net, required for practical realization, is currently under development.

IV. CONCLUSION

We have theoretically investigated the RF performance of mesh reflectors, that are candidates as large lightweight deployable antennas for future space missions. We have shown that the arithmetic pentagonal mesh can decrease unwanted radiation pattern grating lobes by almost 10 dBi compared to a uniform hexagonal mesh. Additionally, we have argued by means of the reflector phase distribution and shown that a shift of the feed closer to the antenna lowers the level of the first sidelobe to that of the nominal paraboloid, and maintains a low level of the grating lobes.

REFERENCES

- [1] 37th ESA Antenna Workshop on Large Deployable Antennas, ESTEC, November 2016.
- [2] T. Orikasa, T. Ebisui, and T. Okamoto, "Sidelobe suppression of mesh reflector antenna by non-regular intervals," in *Antennas and Propagation Society International Symposium. AP-S.*, June 1993, pp. 800–803.
- [3] C. Cappellin, J. R. de Lasson, R. Jørgensen, L. Datashvili, J. Pauw, N. Maghaldadze, M. Migliorelli, and J. C. Angevain, "Large mesh reflectors with improved pattern performances," in *37th ESA Antenna Workshop*, November 2016.
- [4] A. C. Brown, "Irregular segmentation of paraboloidal reflectors," in *Antennas and Propagation Society International Symposium. AP-S.*, July 1996, pp. 242–245.
- [5] GRASP Software, TICRA, Copenhagen, Denmark, www.ticra.com.